Topological Evaluation of Volume Reconstructions by Voxel Carving[☆]

Antonio Gutierrez, Maria Jose Jimenez[*]

Applied Math (I) Department,
University of Seville, Spain

David Monaghan, Noel E. O'connor

INSIGHT Centre for Data Analytics,
Dublin City University, Ireland

Abstract

Space or voxel carving [1, 4, 10, 15] is a technique for creating a three-dimensional reconstruction of an object from a series of two-dimensional images captured from cameras placed around the object at different viewing angles. However, little work has been done to date on evaluating the quality of space carving results. This paper extends the work reported in [8], where application of persistent homology was initially proposed as a tool for providing a topological analysis of the carving process along the sequence of 3D reconstructions with increasing number of cameras. We give now a more extensive treatment by: (1) developing the formal framework by which persistent homology can be applied in this context; (2) computing persistent homology of the 3D reconstructions of 66 new frames, including different poses, resolutions and camera orders; (3) studying what information about stability, topological correctness and influence of the camera orders in the carving performance can be drawn from the computed barcodes.

[☆]Partially supported by the Spanish MEC project MTM2012-32706; The research that led to this paper was supported in part by the European Commission under the Contract FP7-ICT-287723 REVERIE.

[*]Corresponding author

Email addresses: antgutdel@alum.us.es, majiro@us.es (Antonio Gutierrez, Maria Jose Jimenez), {david.monaghan,noel.oconnor}@dcu.ie (David Monaghan, Noel E. O'connor)

Keywords: voxel carving, volume reconstruction, persistent homology, barcodes, evaluation

1. Introduction

Homology is topologically invariant, meaning it is a property of an object that does not change under continuous (elastic) transformations of the object. Roughly speaking, homology characterizes "holes" in any dimension (e.g. connected components, tunnels and cavities in a 3D space). Homology computation can be carried out over a combinatorial structure called *cell complex*, which is built up by basic elements (*cells*) of different dimensions (vertices, edges, faces, etc.). One can take advantage of the combinatorial nature of a digital image (as a set of voxels) to compute homology by taking as input the (algebraic) cubical complex associated to the image. *Persistent homology* [5, 17] studies homology classes and their life-times (persistence) in the belief that significant topological attributes must have a long life-time in a filtration (an increasing nested sequence of subcomplexes). In this paper, we work upon the previous paper of the same authors [8] to apply persistence theory for the evaluation of a 3D reconstruction process, providing a wide experimental support to the initial ideas set down there. We want to clarify that the application described here is not the classical use of persistent homology; it is more an experimental use of it. The reconstruction process, along increasing number of cameras, can be modelled as a suitable input for persistent homology computation, giving the possibility of a topological understanding of the whole process. More specifically, we analyse the *persistence barcodes* [3] which are graphical representations of pairs of birth and death times of homology classes as a collection of horizontal line segments (intervals) in a plane, in order to extract information about the topological evolution of the reconstructions.

In the following Section, we describe the specific context in which we apply persistent homology computation. Section 3 describes the method used to topologically characterise the evolution of the reconstructions by voxel carving with respect to the number of cameras used. Reports on the computations performed as well as some conclusions are collected in Section 4. We draw some ideas for future work in the last Section.

Figure 1: A subject of interest being identified and segmented from the background of the image.

2. Voxel Carving Approach and its evaluation

Space or voxel carving [1, 4, 10, 15] is a technique for creating a three-dimensional reconstruction of an object from a series of two-dimensional images captured from cameras placed around the object at different viewing angles. The technique involves capturing a series of synchronised images of an object, and, by analysis of these images and with prior knowledge of the exact three-dimensional location of the cameras, deriving an approximation of the shape of the object. The general voxel technique proposed in [10] has been modified and adapted to a specific task, as fully detailed in [12, 13]. And it is in fact this specific voxel carving technique that we are evaluating.

In each image in the synchronised set of images, the subject of interest is identified and then segmented from the background of the image. Fig.1 shows an example of a subject of interest in a camera image and the subject segmentation or silhouette extraction, as it is more commonly known. The subject silhouette is segmented from the background by an autonomous adaptive "approximate median" background modelling algorithm. By using an adaptive background modelling algorithm the silhouette extraction process can be made more robust to environmental changes, such as lighting and unwanted background objects. A 3D bounding box is then drawn around the subject's approximate position in 3D space. This bounding box defines a volume that has a corresponding real world three-dimensional coordinate system. This defined volume can be seen in Fig.2.

In the real world coordinate system the approximate subject volume is populated with voxels, that are set at a particular distance apart or spatial resolution, i.e. if the distance between voxels decreases then the spatial resolution increases. From experimental observation, authors in [12] found that

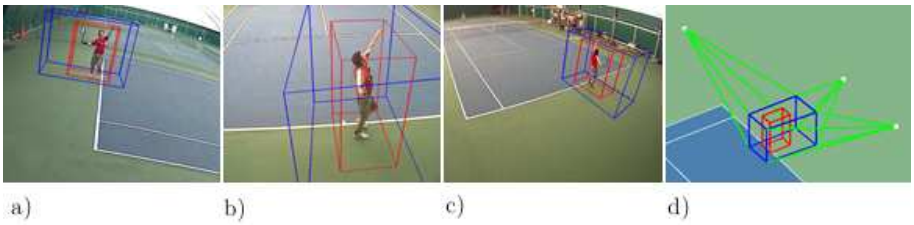

Figure 2: a)-c) shows the subject of interest in 3 different camera views with the red and blue cubes indicating the approximate volume in which the subject exists. d) shows the approximate volume cubes in the corresponding real world coordinate system volume, where the white dots indicate the location of the cameras and the green lines indicate the camera viewpoint or projection direction.

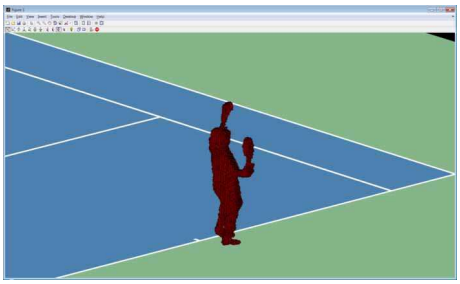

Figure 3: An example of the output of the voxel carving technique when applied to one frame from a tennis match dataset (3DLife ACM Multimedia Grand Challenge 2010 Dataset) [14]

a three dimensional spatial frequency of 4cm, i.e. 15,625 samples per cubic metre, was sufficiently adequate for their purposes. This is based on three premises, (1) the final reconstructions being qualitatively detailed enough to be used as a 3D visualisation tool, (2) the final reconstructions being detailed enough to allow to extract accurate human biomechanical information from the resultant volumes, and (3) based on the computational performance of a single PC this resolution allows to run their algorithm at near to real-time. By using the extracted silhouettes, seen in Fig.1, from each image, inconsistent voxels can be eliminated from the defined volume and by iterating through each of the cameras the remaining voxels in the volume form an approximate 3D representation of the subject.

Voxel carving techniques are very useful for 3D reconstruction as they can cover a very large environment, such as a tennis court, they are non-invasive, they can be implemented with an array of low-cost cameras and the technique

itself is also cheap to compute. However, one of the fundamental difficulties with voxel carving is the unavailability of a ground truth from which to derive the accuracy of the technique. In an attempt to provide some quantitatively evaluation of voxel carving Monaghan et. al. [13] present an evaluation of the technique indirectly via silhouette comparison and in [12] present a method to quantitatively evaluate spatially carved volumetric representations of humans using a synthetic dataset of virtual humans in a tennis court scenario. Such quantification is based on a calculated ground truth and on the computation of Normalised Mean Square Error (NMSE).

From experimental observation the authors found that 50 cameras surrounding a subject could be considered as the maximum number so that the addition of any further cameras would not provide any more accuracy to the final space carving (it should be noted that in a real world scenario having 50 cameras is unrealistic due to costs and physical placements of the cameras). By using the synthetic dataset of virtual humans they created 50 virtual cameras and placed them in the virtual environment surrounding a virtual human. The resultant space carving produced from this ideal setting was then considered to be the ground-truth carving. The NMSE of any reconstruction from a camera setup with fewer than 50 cameras could then be calculated by comparing it to the ground-truth reconstruction, which had been calculated from 50 cameras. The aim of such an evaluation is to somehow quantify the accuracy of the 3D volume produced by the voxel carving process with regard to the number of cameras used. This investigation was motivated by the fact that very little work had been done to date on evaluating the quality of space carving results. A new insight into the voxel carving work by homologically characterising the sequence of reconstruction volumes was initiated in [8]. Given the nature of the carvings, a homology-based approach was presented as a more appropriate mathematical quantification than the relatively simple NMSE-based approach used previously.

3. Persistent Homology for 3D Reconstruction Evaluation

We are concerned with the application of persistent homology computation to provide topological evaluation of the sequence of 3D reconstructions by the voxel carving technique. We consider the whole process of voxel carving with different numbers of cameras as an object with a filtration given by the partial results with each number of cameras. This way, the associated barcode provides a global topological description of the process, that en-

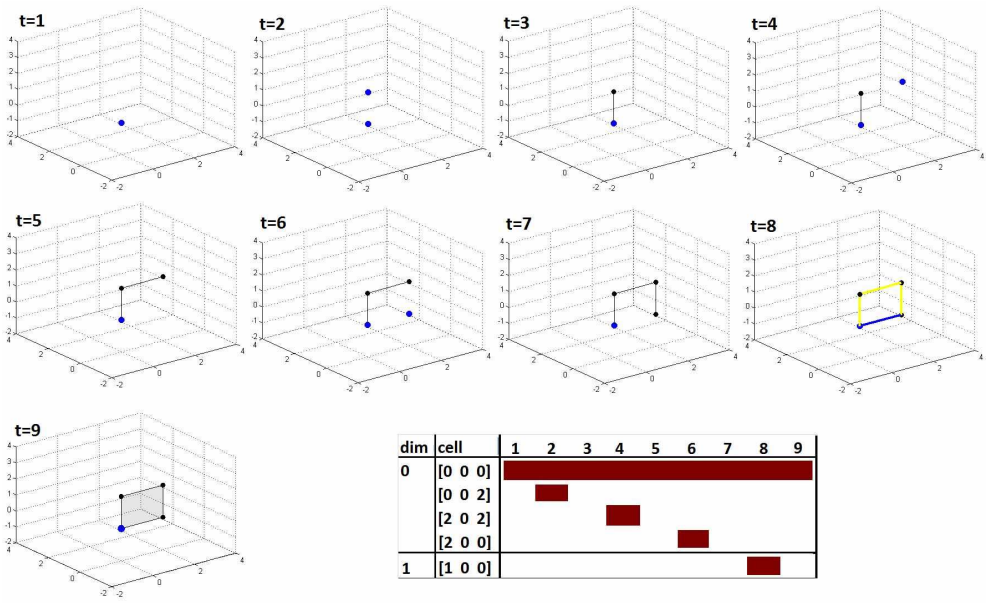

Figure 4: A simple example of computation of persistent homology and the corresponding barcode. Cells are labelled with the time step at which they are added.

riches the numerical comparison against the ground truth model. Although the idea of using persistent homology in this context was first proposed in [8], a more formal and detailed presentation of the method is given in this section. Besides, a considerable amount of experiments presented in next Section, will support the proposed method.

The input data, results of the different voxel carvings, are 3D binary digital images or subsets of points I of $\mathbb{Z}^3$ considered under the $(26, 6)$–adjacency relation for the foreground (I) and background ($\mathbb{Z}^3 \setminus I$), respectively. Due to the nature of our input data, we focus on a special type of cell complex: *cubical complex*. A cubical complex Q in $\mathbb{R}^3$, is given by a finite collection of p-cubes such that a 0-cube is a vertex, a 1-cube is an edge, a 2-cube is a filled square (we call it, simply, a square) and a 3-cube is a filled cube (resp. a cube); together with all their faces and such that the intersection between two of them is either empty or a face of each of them. The cubical complex $Q(I)$ associated to I is given by identification of each 3D point of I with the unit cube centered at that point and then considering all those 3-cubes together with all their faces (square faces, edges and vertices), such that shared faces are considered only once. Sometimes we will refer to p-cubes with the

more general term of *cells* (corresponding to the more general concept of cell complex, see [9]).

Given a cell complex, homology groups can be computed using a variety of methods. Incremental Algorithm for computing AT-model (Algebraic Topological Model) [7], computes homology information of the cell complex by an incremental technique, considering the addition of a cell each time. Once homology of a combinatorial object has been computed, the same algorithm can be used again to update homology information if new cells are added to the existing complex. In [6], the authors revisit this algorithm with the aim of setting its equivalence with persistent homology computation algorithms [5, 17] working over $\mathbb{Z}/2$ as ground ring. We make use of algorithm in [6] for the persistent homology computation (though any other algorithm for computing persistent homology, adapted to cubical complexes, could have been applied).

Denote by R_k the 3D reconstruction (or 3D binary digital image) obtained using k cameras, that is, R_0 represents the initial 3D bounding box, R_1 the set of points obtained after the voxel carving of R_0 with one camera, and so on.

Notice that, every time a new camera is added and the corresponding carving is performed, some points (if any) are removed from the previous reconstruction, so $R_k \supseteq R_{k+1}$. That is, we have a nested sequence of 3D reconstructions with decreasing number of cameras,

$$R_n \subseteq R_{n-1} \subseteq \cdots R_1 \subseteq R_0 \,.$$

Now, associate a cubical complex to each reconstruction as explained above. The following proposition holds.

Proposition 1. Denote by C_{n-k} the cubical complex associated to the reconstruction with k cameras R_k $(k = 0, \ldots n)$. Then, the cubical complex $\mathcal{C} = \{C_i\}_{i=0\ldots n}$ is a filtered complex with the filtration

$$C_0 \subseteq C_1 \subseteq \cdots C_{n-1} \subseteq C_n \,.$$

Obviously, inclusion relation between the complexes is induced by the ones between corresponding reconstructions.

So persistent homology of the filtered complex $\mathcal{C}$ can be considered. Notice that C_i is obtained from C_{i-1} by adding some cubes, together with all

their faces in the cubical complex. The addition of all these cells is accomplished in an order $(c_i^1, \ldots, c_i^{m_i})$ such that if c^j is a face of c^l, then $j < l$. Such an ordering gives place to a new filtration $\mathcal{C}_i$:

$$C_{i-1} \subseteq C_{i-1} \cup \{c_i^1\} \subseteq \cdots \subseteq C_{i-1} \cup \{c_i^1, \ldots, c_i^{m_i}\} = C_i \,.$$

Persistent homology can be computed through this filtration between C_{i-1} and C_i, providing all the pairs of cells responsible for the creation/destruction of homology classes along the process, what allows to construct a "partial" barcode corresponding to the persistent homology of the filtration $\mathcal{C}_i$.

See Fig.4 as a simple example of computation of persistent homology and the corresponding barcode, which represents graphically the birth and death of homology classes along the process.

However, regarding the computation of a barcode associated to the whole filtration $\mathcal{C}$, consider the following definition:

Definition 1. Given a filtered complex $\mathcal{C} = \{C_i\}_{i=0\ldots n}$, such that for each index i, there is a filtration $\mathcal{C}_i$ of complexes $C_i^0 = C_{i-1} \subseteq C_i^1 \subseteq \cdots \subseteq C_i^{m_i} = C_i$, a *simplified barcode* for $\mathcal{C}$ with respect to the filtrations $\mathcal{C}_i$ is the one computed from the barcode of $\mathcal{C}$ after taking these operations, for each i:

1. all the homology classes living at time $i-1$ in the filtration $\mathcal{C}$ that are destroyed at a certain time j of the filtration $\mathcal{C}_i$, with $j = 1 \ldots m_i$, are set to die at time i in the filtration $\mathcal{C}$;
2. all the homology classes that are created at a certain time j of the filtration $\mathcal{C}_i$, with $j = 1 \ldots m_i$, are set to be born at time i in the filtration $\mathcal{C}$;
3. all the homology classes that are created at a certain time j of the filtration $\mathcal{C}_i$, with $j = 1 \ldots m_i$ and destroyed at time l of the filtration $\mathcal{C}_i$, with $l = 2 \ldots m_i$ and $j < l$, are eliminated from the barcode.

Hence, in the simplified barcode, creation and destruction of homology classes are only considered to happen between two consecutive number of cameras and not in the increasing process between them. So, "small" elements of homology, like those in Fig.4, are not represented. This barcode will help to visualize the whole computation in order to easily analyze the behaviour of the elements of homology.

Proposition 2. The simplified barcode of the filtration $\mathcal{C} = \{C_i\}_{i=0\ldots n}$ described above with respect to the filtrations

$$C_{i-1} \subseteq C_{i-1} \cup \{c_i^1\} \subseteq \cdots \subseteq C_{i-1} \cup \{c_i^1, \ldots, c_i^{m_i}\} = C_i$$

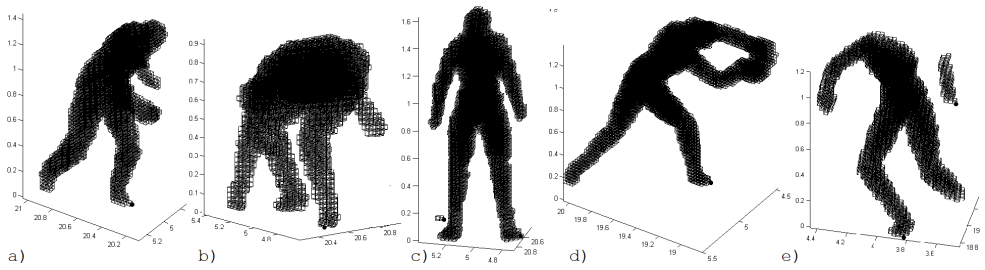

Figure 5: Different 3D reconstructions with 43 cameras and resolution 0.027 illustrating the variety in poses of the subject.

is independent of the order taken for the cells $\{c_i^1, \ldots, c_i^{m_i}\}$ added betweeen each two consecutive subcomplexes C_{i-1} and C_i, for $i = 1 \ldots n$.

Notice that the order in which the cells are considered to compute persistent homology between two subcomplexes C_{i-1} and C_i could lead to different barcodes. By setting the times of birth or death to the interval ends in each filtration $\mathcal{C}_i$, we achieve a representation tool (the simplified barcode) that depends exclusively on the camera orders taken for the reconstructions.

4. Experimental results

Apart from 5 different frames (of resolution 0.040) used in [8] for computation, we have taken as input 22 new frames extracted from a 3D video sequence of a subject with different poses (see Fig.5 for some examples), including poses in which a loop was formed by the arms of the subject (Fig. 5 d)), and with three different voxel resolutions: 0.040, 0.034 and 0.027, that is, a total of 66 new frames. By resolution 0.040, we mean that the spacing between each voxel is 4 cm in the OX, OY and OZ directions, what means $15,625$ voxels per cubic metre.

A general perception is that representation of a subject in an upright pose with the arms quite separated from the body produce simpler barcodes while more complex poses (like the one in Fig.5 b)) give place to more complex homological information that hardly find stabilization along time (number of cameras).

Fig.6 shows a case of simple pose for which the carving process stabilizes at 6 cameras (with a unique connected component); several tunnels have been living from 1 to 3 cameras. That means that, in order to produce a topologically correct model, at least 6 cameras are needed in this case. However,

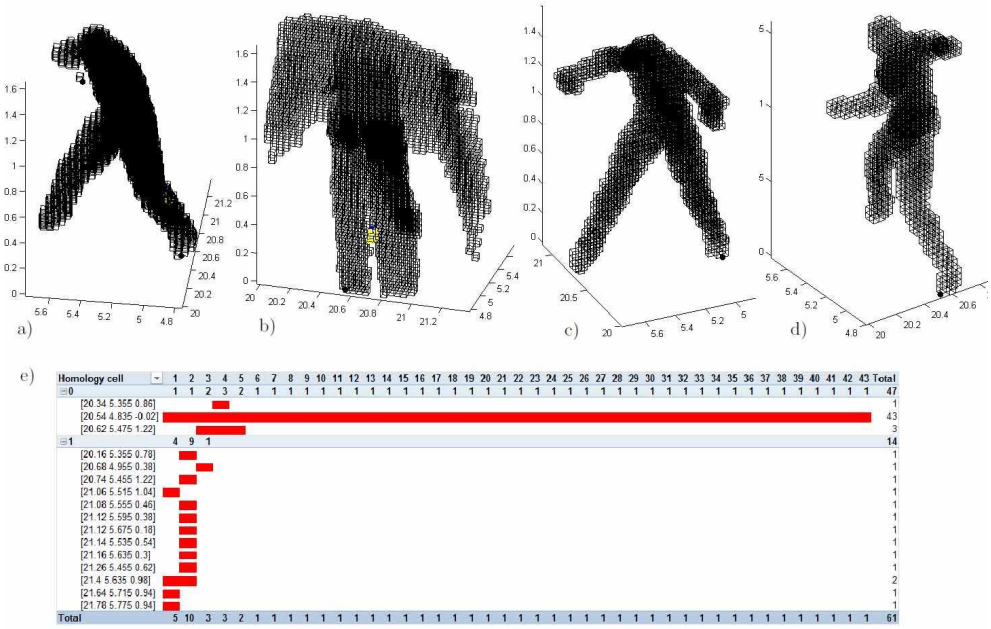

Figure 6: 3D Reconstructions of resolution 0.040 using a) and b) 3 cameras with two different view angles, c) 6 cameras, d) 43 cameras, what is considered the ground-truth model. e) Barcode associated to the whole sequence of 3D reconstructions with increasing number of cameras (from 1 to 43).

Fig.7 reflects a not so complex pose but with the handicap of having enough proximity between arms and body to find it difficult to stabilize. Notice the more complex barcode associated (in which 4 connected components and 29 tunnels are represented) and, especially, the fact that new 1–homology classes are created with high number of cameras, what shows inestability in the process.

Based on our experiments, we have taken different observations with regard to the following aspects:

- *Topological correctness.* By this method, we can topologically control the reconstructed models and estimate a minimum number of cameras needed to get a topologically correct 3D model. It also provides important feedback to the algorithm effectively used for the carving performances.

  Although all the reconstructed volumes were supposed to represent a connected object, 15 out of 66 frames stabilize towards a model with

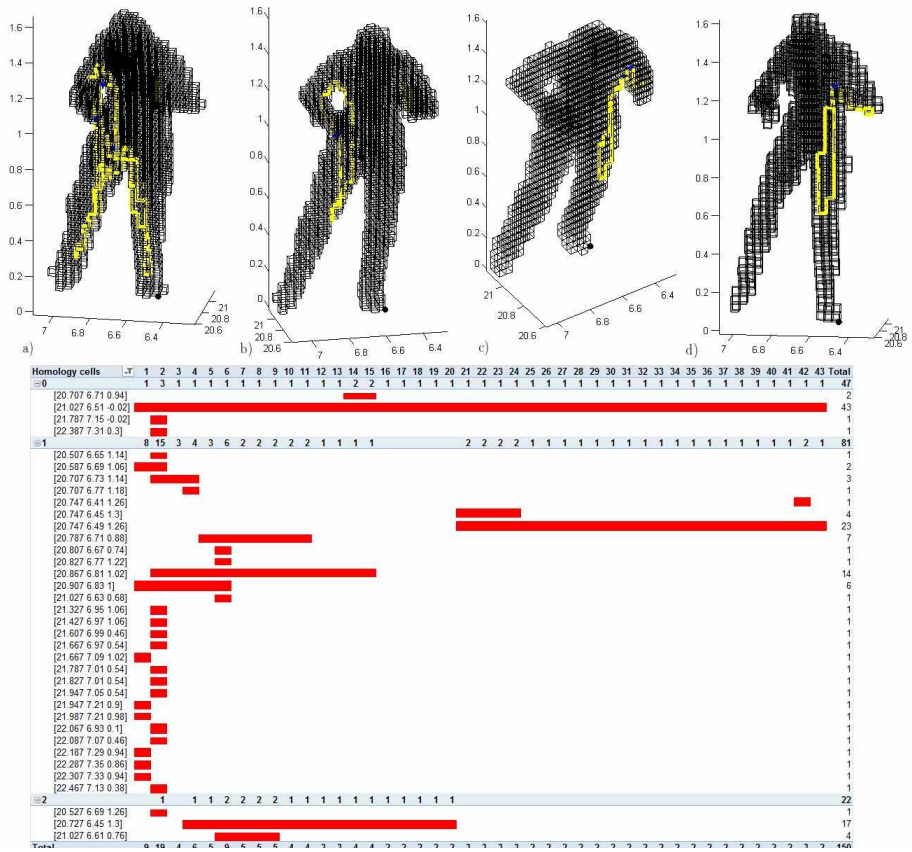

Figure 7: 3D Reconstructions (viewed from different angles) using different number of cameras: a) 6 cameras, b) 14 cameras, c) 22 cameras and d) 43 cameras (ground-truth model). Representative cycles of homology are highlighted. Below, barcode associated to the whole sequence of 3D reconstructions from 1 to 43 cameras.

more than one connected component. By taking an a posteriori analysis of those models we find that more than one 0-homology classes persist when one of the following facts occur:

1. Part of the background is wrongly considered as being part of the foreground for the reconstruction (see Fig.5 c)). These cases (4 in total) may be caused by a deficient silhouette extraction, though this is only an assumption derived from the visualization.
2. Part of the body is not reconstructed and hence, it results in a "broken" model (see Fig.5 e)). The reason may lie in a bad positioning of the initial bounding box as it can be supposed from

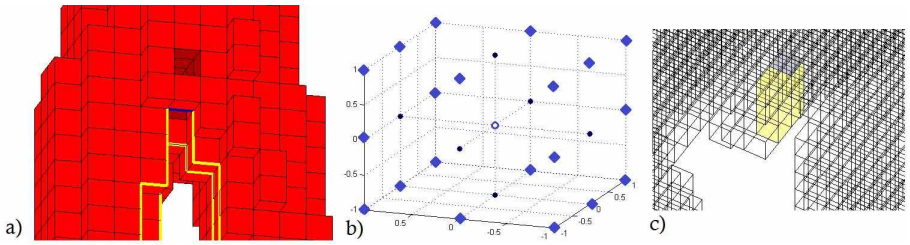

Figure 8: a) A "little" tunnel from the surface of a reconstruction that persists until the maximum number of cameras. b) A cavity may be produced in a reconstruction by a missed point (○), if the 6-adjacent points (●) belong to the representation; the rest of the 26-adjacent points (◇) can either belong or not to the representation. c) Detail of a reconstruction with a representative cycle of 2-homology highlighted.

a visual inspection.

Regarding 1-homology classes, expected evolution of tunnels are due to junctions between two parts of the body (for example, as in Fig.7 a), b)), which stabilize disappearing with appropriate camera views (with 16 cameras in the example). However, there are some cases of persistence of tunnels that lead to think of numerical errors in the computations made for the carvings. A close inspection of the representative cycles computed by the Incremental AT-model Algorithm reveals that they are, in fact, little tunnels formed from the surface of the model, that should not logically live there (see Fig.8 a)).

We also computed several frames in which a loop was formed by the arms of the subject (like in Fig. 5 d)). The tunnel was correctly detected, in about the 79 per cent of cases, with no more than 6 cameras.

As for homology classes of dimension 2, due to the nature of the voxel carving process, only voxels on the surface of the object were expected to be removed each time, giving place to different connected componentes and tunnels, but not to cavities. However, a high number of cavities are found in the output results (as in Fig.7). Technically, "small" cavities might occur (see Fig.8 b), c)) near the surface, since the projection of the silhouette over the volume (to determine points to be deleted) could exclude a point, but not its 6-adjacent points. Nevertheless, the persistence or birth of 2-homology classes at high number of cameras also point out to the possibility of numerical errors in the specific technique used.

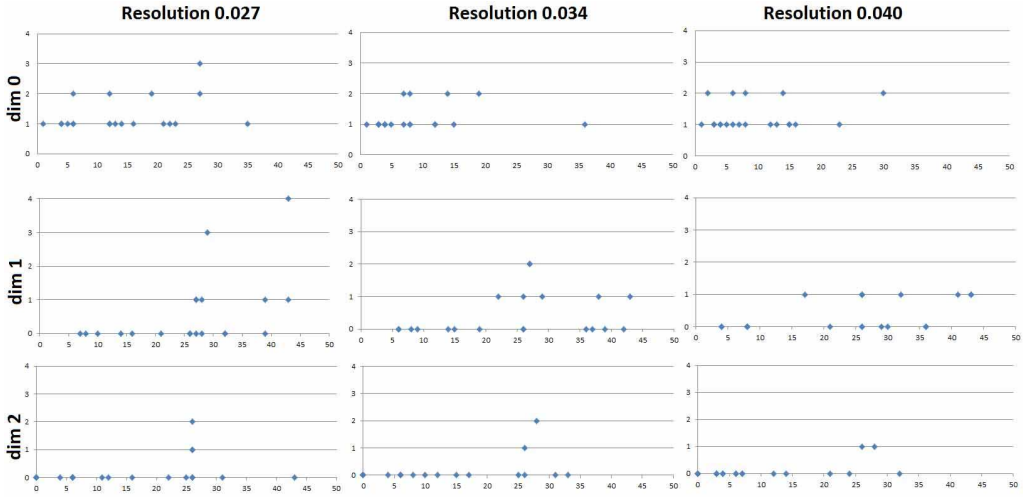

Figure 9: For each resolution (column) and each dimension i (row), representation of the pairs (n_i, β_i), where n_i is the number of cameras at which the corresponding Betti number β_i stabilizes.

- *Stability.* By this evaluation, we can set the minimum number of cameras needed to obtain a 3D model whose homology classes persist until the maximum number of cameras, that is, a stable model. Regarding 0-homology classes, graphics at first row of Fig.9 collects, for each resolution, the pairs (n_0, β_0), where n_0 (horizontal axis) is the minimum number of cameras from which β_0, Betti number of dimension 0 (on the vertical axis) stabilizes, or even more, no more 0-homology classes are created or destroyed along the increasing number of cameras. On average, β_0 stabilizes at 11 cameras, with a standard deviation of 8. As for β_1, data represented in second row of Fig.9 reflect higher dispersion, with a mean of 25 cameras and standard deviation of 12, what shows higher inestability of the models with respect to the creation/destruction of tunnels. These statistics have been followed with low deviation in the cases of poses including a loop, what does not seem to infere worse stability to the models. Cavities usually live (shortly) at low dimensions, though, as it can be appreciated in the third row of Fig.9, several models find also stabilization of β_2 at high number of cameras, yielding to a mean of 13 and standard deviation of 12 cameras.

- *Resolution.* The increase of spatial resolution implies in general a more

complex barcode in the sense of an important increase in the number of homology classes (bars in the barcodes), mainly of dimensions 1 and 2, living (with any persistence) along the process. In fact, the mean of number of 0-homology classes in resolutions 0.04, 0.034 and 0.027, are 4.6, 4.9 and 7, respectively; for dimension 1, the averages lie around 30, 36 and 43; for dimension 2, 10.7, 11.3 and 14.4. However, based on experience, we can assure that there is no meaningful improvement in using higher spatial resolutions with respect to either stability of the reconstructed models along the number of cameras or topological correctness of the models. On the contrary, lower resolution in general leads to a simpler barcode and hence, a more reliable model from a topological viewpoint.

- *Camera order.* The outcome of the voxel carving method is clearly dependent on the camera order taken, so an important aspect to consider is the influence of this order in the performance of the carvings. There are some works in the literature ([11, 16], among others) that address the problem of planning next view in a context of getting a shape from silhouette (as it is also called the space carving method) with minimal different views. The main idea in those papers could be interpreted in our context as taking, each time, the camera that produces the silhouette that differs the most from the previous one. In the search of a strategy for a good positioning of cameras, we used this premise to produce what we called the *optimum* order. Then, our aim was to find out if the use of the considered optimum order had a direct reflection on a faster stability or higher topological correctness of the reconstructed 3D models. We computed voxel carving of all the 22 different frames under different orders of the cameras used (sequential, optimum and other randomly choosen orders). On the base of the experiments, the sequential order emerged as a quite worse choice than any other order used. In most cases, this order presented a more complex barcode (see Fig.11 as an example of comparison) in the sense of being less topologically correct at any time and having worse stability of the models along time. This way, taking sequential, optimum and other 2 random orders, and the corresponding histograms (or vectors collecting the number of homology classes at each time), the computation of the average histogram for each order gives an idea of the general tendency of homological elements along time. Fig.10 displays a graph where

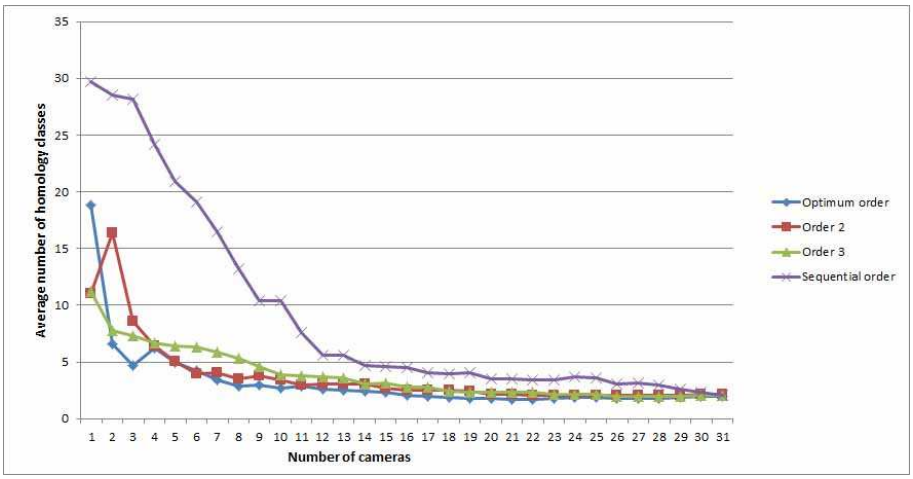

Figure 10: Representation of average histograms obtained from 10 different frames computed

these average histograms are represented, showing the differentiated behaviour of the computation under sequential order against others. However, random and optimum cases are similar, what strengths the hypothesis that we can produce moderately high quality voxel carving using only a few cameras chosen randomly (but not sequentially).

5. Conclusions and Future Work

The new insight developed in this paper to evaluate a voxel carving technique significantly enriches the evaluation made in [12] by means of NMSE quantification. Although this is not the standard use of persistent homology, the experimentation carried out has provided valuable information from a topological point of view of the reconstructions process.

We propose here different research lines for future.

Experimentation with other complexes. One could consider other filtrations on the set of reconstructions that could allow different computations. For example, the Differences Complex: for each reconstruction by voxel carving and for each number of cameras R_i, take the voxels that are left to be deleted with respect to the ground truth (R_n), $L_i = R_i \setminus R_n$. Consider, then the associated cubical complexes or difference complexes, $\{D_i\}_i$ to each set of 3D points L_i. Notice that L_i is a cubical complex given by the 3-cubes that

Figure 11: Two barcodes associated to the reconstruction of a same frame with two different camera orders: the theoretically optimum and the sequential order.

belong to C_i (cubical complex associated to R_i) but not to C_{i-1} together with all their faces (see Fig.12 a)-e)). Hence, a new filtration is given

$$D_{n-1} \subseteq D_{n-2} \subseteq \cdots \subseteq D_1 \subseteq D_0$$

and persistent homology can be computed. The computations made of the corresponding simplified barcode, as defined in Section 3, have shown a high increase in the number of homology classes with respect to the former computations (Fig.12), what could provide different information about the whole process that might complement the one given by the reconstructions themselves.

Video sequences. An interesting question arises by fixing a certain number of cameras and considering the sequence of 3D reconstructions along time in a video. Holes can be produced along time by different movements of the body that should not be stable along the complete scene, so the homological analysis of voxel carving performance of video sequences could shed some light on the classification of these movements. Zigzag persistence [2] seems to be a more appropriate context for this application.

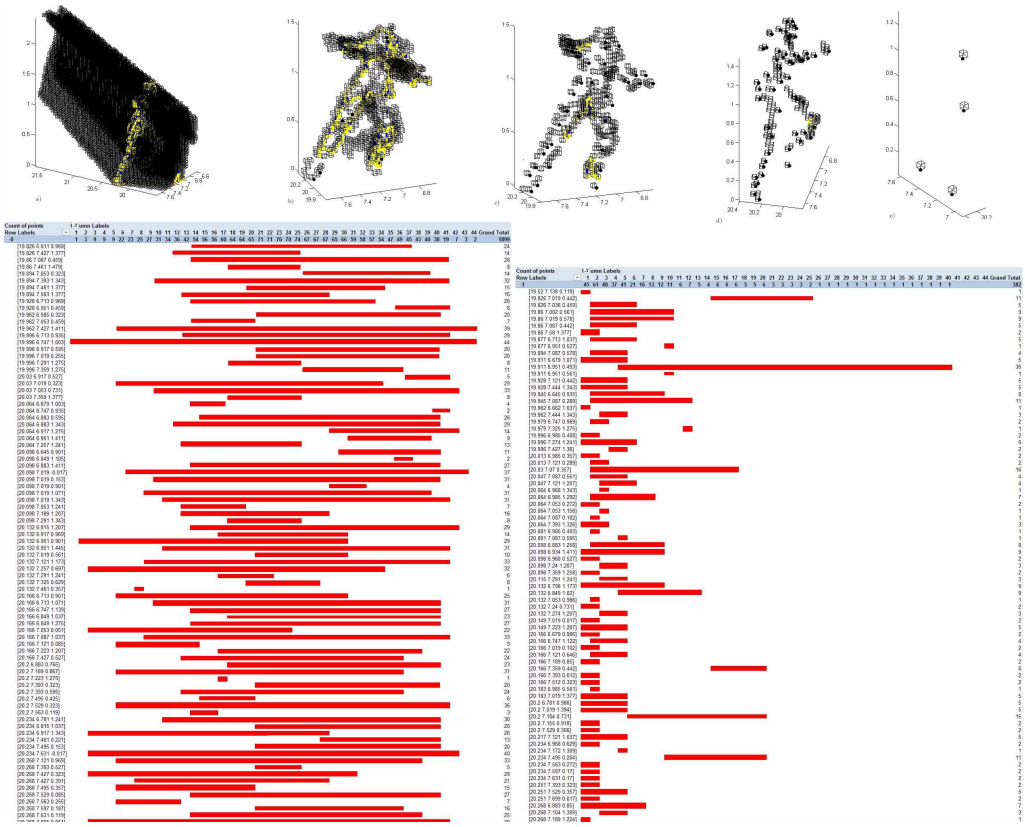

Figure 12: Differences with respect to the ground-truth model of reconstructions of a frame (viewed from different angles) using different number of cameras: a) 1 cameras, b) 3 cameras, c) 12 cameras, d) 32 cameras, e) 42 cameras. Representative cycles of homology are highlighted. Below, barcodes associated to the whole sequence of differences from 1 to 43 cameras.

Acknowledgments

The authors wish to thank Dr. Rocio Gonzalez-Diaz and Prof. Walter Kropatsch for the useful discussions related to the topic of this paper, as well as the reviewers for their valuable comments.

References

[1] Broadhurst, A., Drummond, T., Cipolla, R.: A probabilistic framework for space carving. In: Conf on Computer Vision, 1, pp. 388 (2001)

[2] Carlsson G., de Silva V., Morozov D.: Zigzag persistent homology and real-valued functions. SoCG'09. ACM, New York, NY, USA, 247-256 (2009)

[3] Collins A., Zomorodian A., Carlsson G., Guibas L.: A barcode shape descriptor for curve point cloud data. Computers and Graphics 28 (2004) 881–894

[4] Culbertson,W. B., Malzbender, T., Slabaugh, G.: Generalized voxel coloring. In: Intern. Workshop on Vision Algorithms: Theory and Practice, pp. 100-115 (1999)

[5] Edelsbrunner H., Letscher D., Zomorodian A.. Topological persistence and simplification. FOCS '00, IEEE Computer Society, 454–463 (2000)

[6] Gonzalez-Diaz, R., Ion, A., Jimenez, M. J., Poyatos, R.: Incremental-Decremental Algorithm for Computing AT-Models and Persistent Homology. In: A. Berciano et al. (Eds.) CAIP 2011. LNCS vol. 6854, pp. 286–293. Springer, Heidelberg (2011)

[7] Gonzalez-Diaz R., Real P.: On the cohomology of 3D digital images. Discrete Applied Math 147 (2-3), 245–263 (2005)

[8] Gutierrez A., Monaghan D., Jimenez M.J. and O'Connor N.E.: Persistent Homology for 3D Reconstruction Evaluation. In: M. Ferri et al. (Eds.): CTIC 2012, LNCS 7309, pp. 30–38, 2012

[9] Hatcher A.: Algebraic Topology. Cambridge University Press (2002)

[10] Kutulakos, K. N., Seitz, S. M.: A theory of shape by space carving. Intern. Journal of Computer Vision. 38, 199–218 (2000)

[11] Maver, J.; Bajcsy, R.:Occlusions as a guide for planning the next view. IEEE Transactions on Pattern Analysis and Machine Intelligence, 15 (5), 417- 433 (1993)

[12] Monaghan, D., Kelly, P., O'Connor, Noel E.: Quantifying Human Reconstruction Accuracy for Voxel Carving in a Sporting Environment. In: ACM MM, 28 Nov - 1 Dec. 2011, Scottsdale, AZ.

[13] Monaghan, David and Kelly, Philip and O'Connor, Noel E. Dynamic voxel carving in tennis based on player localisation using a low cost camera network In: 2011 IEEE International Conference on Image Processing (ICIP 2011), Brussels, Belgium, 11-14 Sept. 2011

[14] Ciaran O' Conaire and Philip Kelly and Damien Connaghan and Noel E. O'Connor: TennisSense: A Platform for Extracting Semantic Information from Multi-camera Tennis Data. In: DSP 2009 - 16th International Conference on Digital Signal Processing, 1062–1067 (2009)

[15] Seitz, S. M., Curless, B., Diebel, J., Scharstein, D., Szeliski, R.: A comparison and evaluation of multi-view stereo reconstruction algorithms. In: IEEE Conference on Computer Vision and Pattern Recognition, 1, pp. 519-528 (2006)

[16] Sablatnig, R.; Tosovic, S.; Kampel, M.: Next view planning for a combination of passive and active acquisition techniques. In: Fourth International Conference on 3-D Digital Imaging and Modeling, 2003. 3DIM 2003. Proceedings. 62– 69 (2003)

[17] Zomorodian A., Carlsson G.: Computing persistent homology. Discrete and Computational Geometry 33 (2), 249-274 (2005)